Extracellular RNA mediates endothelial-cell permeability via vascular endothelial growth factor

Silvia Fischer,[1,2] Tibo Gerriets,[3,4] Carina Wessels,[3] Maureen Walberer,[3,4] Sawa Kostin,[5] Erwin Stolz,[3,4] Kirila Zheleva,[1] Andreas Hocke,[6] Stefan Hippenstiel,[6] and Klaus T. Preissner[1]

[1]Department of Biochemistry Medical School, Justus-Liebig-University, Giessen; [2]Department of Anesthesiology, Department of Experimental Neurology, Kerckhoff-Klinik, Bad Nauheim; [3]Department of Neurology, Medical School, Justus-Liebig-University, Giessen; [4]Department of Radiology, Department of Experimental Neurology, Kerckhoff-Klinik, Bad Nauheim; [5]Core Lab for Molecular and Structural Biology, Max-Planck-Institute for Heart and Lung Research, Bad Nauheim; [6]Charité–Universitätsmedizin, Department of Internal Medicine/Infectious Pulmonary Diseases, Berlin, Germany

Cell injury leads to exposure of intracellular material and is associated with increased permeability of vessels in the vicinity of the damage. Here, we demonstrate that natural extracellular RNA as well as artificial RNA (poly-I:C), or single-stranded RNA but not DNA, significantly increased the permeability across brain microvascular endothelial cells in vitro and in vivo. RNA-induced hyperpermeability of tight monolayers of endothelial cells correlated with disintegration of tight junctions and was mediated through vascular endothelial growth factor (VEGF), reminiscent of heparin's activities. Antisense oligonucleotides against VEGF-receptor 2 (VEGF-R2) prevented the permeability-inducing activity of extracellular RNA and heparin completely. Hence, these polyanionic substances can lead to mobilization/stabilization of VEGF with the subsequent activation of VEGF-R2. In accordance with these functional data, strong binding of VEGF as well as other growth factors to RNA was demonstrable. In in vivo rat models of $FeCl_3$-induced sinus sagittal is superior thrombosis and stroke/brain edema, pretreatment of animals with RNase (but not DNase) resulted in a significant reduction of vessel occlusion, infarct volume, and prevention of brain edema formation. Together, these results identify extracellular RNA as a novel natural permeability factor, upstream of VEGF, whereas counteracting RNase treatment may serve as new vessel-protective modality. (Blood. 2007;110:2457-2465)

Introduction

Brain homeostasis is maintained by the blood-brain barrier (BBB), which forms a mechanical and functional threshold between the central nervous system and the systemic circulation. The barrier is relatively impermeable to ions, many amino acids, small peptides, and proteins, and thus contributes to the maintenance of a specific neural tissue environment. In vertebrates, the BBB exists at the level of the endothelial cells that form brain capillaries[1] in order to regulate and limit the degree of trans- and paracellular flux.[2] The tight barrier properties of the BBB result from the absence of fenestrations, the low number of pinocytotic vesicles, and the presence of tight intercellular junctions between endothelial cells with extremely high electrical resistance.[3]

Pathologic conditions associated with brain tumors, head injury, or ischemic stroke are accompanied by endothelial-cell dysfunction, leading to increased permeability across the BBB, which might lead to the development of vasogenic cerebral edema.[4,5] Vascular endothelial growth factor (VEGF) as a hypoxia/ischemia inducible protein in vitro and in vivo is one of the strongest natural permeability factors[6] and a likely candidate for the development of ischemia- and tumor-induced vasogenic brain edema.[7-9] VEGF stimulates endothelial-cell growth and migration in vitro[10,11] and angiogenesis in vivo.[6,12] VEGF was originally described as a potent vascular permeability factor responsible for the accumulation of plasma protein–rich fluid in the ascites of patients with tumors.[13] Structurally, VEGF exists as a dimeric glycoprotein of molecular weight (Mr) 34 000 to 42 000 and is related to the platelet-derived growth factor family of molecules.[14] Although VEGF is the product of a single gene, 6 differentially spliced isoforms between 121 and 206 amino acid residues exist in humans[15,16] that exhibit similar functional activities. Different isoforms are distinguished by their affinity for heparin: although $VEGF_{121}$ does not bind heparin, $VEGF_{165}$ has moderate affininity for heparin, whereas $VEGF_{189}$ and $VEGF_{206}$ bind heparin with high affinity.[17] VEGF exerts its multiple actions by ligation with tyrosine kinase receptors, VEGF-receptor 1 (VEGF-R1), as well as VEGF-R2,[18-20] which are expressed on vascular endothelial cells. A third member, VEGF-R3 is expressed on lymphatic endothelial cells.[21]

During pathologic conditions of the brain associated with tumor burden, stroke, or head injury, nucleic acids might be released by damaged cells. RNA-proteolipid complexes were detected in the circulation of patients with cancer and were suggested to represent a specific secretory product of cancer cells.[22] Accordingly, circulating RNA is present in blood plasma of patients with tumors.[23] The presence of specific types of RNA in a variety of cancer types proved to be useful in cancer diagnosis.[24,25] It has been postulated that extracellular RNA and DNA are not inert molecules, but contain biological activities.[26] Our group has identified extracellular RNA for the first time as a specific cofactor of the serine protease factor VII–activating protease,[27] and as potent cofactor for the contactphase of intrinsic blood coagulation (C. Kannemeier et

Submitted August 9, 2006; accepted June 7, 2007. Prepublished online as *Blood* First Edition paper, June 19, 2007; DOI 10.1182/blood-2006-08-040691.

The online version of this article contains a data supplement.

The publication costs of this article were defrayed in part by page charge payment. Therefore, and solely to indicate this fact, this article is hereby marked "advertisement" in accordance with 18 USC section 1734.

al, unpublished results, March 2003). Until now, there has been no information about other functional activities of extracellular RNA. Despite the presence of RNases in the circulation, some RNA species seem to be protected against degradation.[28]

Based on these previous data and considerations, here we first demonstrate cellular activities of extracellular RNA in that natural and artificial RNA provoked hyperpermeability of brain-derived endothelial cells, leading to significant elevation of flux and disintegration of tight junctions. RNA-mediated permeability changes were caused via the mobilization/activation of VEGF and by its interaction with VEGF-R2. Interestingly, RNase treatment in rat models of sinus thrombotic occlusion and focal cerebral ischemia significantly reduced the degree of vessel occlusion and vasogenic brain edema. These data provide compelling evidence for a novel function of extracellular RNA in inducing vessel permeability, upstream of VEGF, whereby an effective antagonistic function of exogenous RNase is described.

Materials and methods

Materials

Poly-I:C was purchased from Amersham-Pharmacia (Braunschweig, Germany); heparin, the nucleotide monophospate mixture, and the monoclonal antibody against α-actin were from Sigma (Munich, Germany); RNase and DNase were from Fermentas (St Leon-Rot, Germany); RNase inhibitor was from Calbiochem (Schwalbach, Germany); single-stranded RNA (ssRNA) was from invivoGen (Toulouse, France); VEGF and the polyclonal antibody against human VEGF were from PeproTech (London, United Kingdom); the antisense oligonucleotides against VEGF-R1 and VEGF-R2 were from Carl-Roth (Karlsruhe, Germany); antibodies against ZO-1, ZO-2, claudin 5, and VE-cadherin were from Zymed (Berlin, Germany); and cell culture medium was from GIBCO (Karlsruhe, Germany). The signaling inhibitors wortmannin, PD989959, SB203580, SB600125, and 2-aminopurine were from Calbiochem (Darmstadt, Germany); and N^G-monomethyl-L-arginine (NMMA) was from Biotrend (Cologne, Germany).

Cell culture

Capillary brain-derived microvascular endothelial cells (BMECs) were isolated and cultured as described.[29] CSG 120/7 cells (carcinoma submandibular gland cells) were cultured in Dulbecco modified Eagle medium (DMEM) supplemented with 10% (vol/vol) fetal calf serum (FCS), 200 U/mL penicillin, and 200 U/mL streptomycin. Before the experiments, cells were washed once with phosphate-buffered saline (PBS) and incubated for the indicated time periods in cell culture medium containing the different agents at the indicated concentrations.

Analysis of endothelial monolayer permeability

BMECs or CSG cells were cultured to confluency on collagen-coated polycarbonate membranes. Permeability across the cell monolayer was analyzed as described previously.[29]

Antisense oligonucleotide treatment

BMEC monolayers were treated 48 hours before the start of the experiment with antisense oligonucleotides containing sequences complementary to bovine VEGF-R1 and mouse VEGF-R2 mRNA (GenBank accessionnumbers X94263 and 70842). VEGF-R1 antisense, 5′-CAAAGATGGACTCGGGAG-3′; and VEGF-R2 antisense, 5′-CCCACAGAGGCGGCTCGG-3′. Two scrambled sequences were used as negative controls: scrambled VEGF-R1, 5′-AGCTAGGCACGAGAGTGA-3′; and scrambled VEGF-R2, 5′-CACAGCGAGGCGGCTCCG-3′. The cellular uptake of these oligonucleotides was confirmed using fluorescence microscopy inspection by using the respective Cy3–5′ end–modified oligonucleotides.

Isolation of cellular RNA and DNA

Total RNA and DNA were isolated from confluent cultures of smooth muscle cells and BMECs using an extraction kit (Sigma) or the DNAzol reagent (Invitrogen, Groningen, the Netherlands). Cells were washed once with PBS and extraction was performed according to the manufacturer's instructions. Quality of total RNA and DNA were confirmed by electrophoresis on 1% agarose gel followed by ethidium bromide staining. Total RNA was quantified using a Gene Quant photometer (Amersham Pharmacia).

Immunofluorescence microscopy

BMECs were grown either on normal Biocoat petri dishes (BD Biosciences, Munich, Germany) or on plastic slides and treated as described. For staining, monolayers were washed twice with PBS, fixed in 1% paraformaldehyde at 4°C for 15 minutes, washed with PBS, permeabilized with 0.05% Triton for 10 minutes, and washed again 5 times with PBS. Specimen were blocked with 10% normal goat serum (Sigma) at 22°C for 30 minutes, followed by incubation with 1:50 or 1:100 diluted rabbit-polyclonal antibodies against occludin, ZO-2, ZO-1, claudin-5, or VE-cadherin, respectively. After washing with PBS, cells were incubated at 22°C for 1 hour with Cy3-conjugated goat anti-rabbit IgG (dilution 1:400) followed by washing. Specimens were inspected with the help of a fluorescent photomicroscope (Leica, Bensheim, Germany).

Binding of biotinylated RNA to VEGF

Microtiter plate wells were coated each with 50-μL solutions of $VEGF_{165}$, $VEGF_{121}$, platelet-derived growth factor, placenta growth factor-1, basic fibroblast growth factor, or bovine serum albumin (BSA; 10 μg/mL each) in 100 mM sodium carbonate (pH 9.5) at 4°C for 20 hours. Wells were washed and blocked with TBS containing 3% BSA for 2 hours. Different concentrations of biotinylated RNA (3.1-50 μg/mL), prepared from RNA using the Psoralen-PEO-Biotin reagent (Pierce, Rockford, IL), were allowed to bind at 22°C for 2 hours followed by 3 washings with TBS. Bound biotinylated RNA was detected using peroxidase-conjugated streptavidin (Dako, Glostrup, Denmark) and the immunopure TMB (3,3′,5,5′-tetramethylbenzidine) substrate kit (Pierce) by measuring the reaction products at 450 nm. In competition binding assays, biotinylated RNA was mixed with unlabeled RNA or heparin in different molar ratios.

Sinus sagittalis superior thrombosis in rats

In 48 male Sprague-Dawley rats (weight between 271 and 359 g), $FeCl_3$-induced superior sagittalis sinus thrombosis was performed as described previously.[30] All procedures were carried out with approvement of the appropriate authority for animal protection. In 4 experimental groups with 12 animals each, 100 μL each of isotonic saline (control), RNase and DNase (1 mg/mL each), heparin, (100 μg/mL, 100 IU/kg body weight; Aventis, Germany), VEGF-antibody (Roche, Grenzach-Wyhlen, Germany), or factor XIIa inhibitor H-D-Pro-Phe-Arg-chloromethylketone (Bachem, Basel, Switzerland), both 10 mg/kg body weight, were administered 30 minutes prior to induction of cerebral sinus thrombosis via a femoral vein. In all animals, mean arterial blood pressure was monitored continuously during operation and drug infusion. Partial pressures of CO_2 and O_2, pH, and blood glucose were determined before and 30 minutes after craniotomy and superior sagittalis sinus occlusion. Bleeding time was measured before as well as 30 minutes and 24 hours after drug application. At 24 hours after induction of superior sagittalis sinus thrombosis, rat brains from each treatment group were removed, fixed in 4% paraformaldehyde, dehydrated, and embedded in paraffin using standard techniques. Sections (5 μm) were stained with hematoxylin-eosin using standard techniques. The remaining animals were subjected to magnetic resonance imaging (MRI; 7 T PharmaScan; Bruker, Ettlingen, Germany; 7.0 T, 300.51 MHz for ^1H, 300 mT/m self shielding gradient system). Imaging was performed immediately after sinus occlusion and repeated on the first and seventh postoperative days. The imaging protocol included a venous 2D time-of-flight MR-angiography sequence (slice thickness, 0.3 mm; field of vision [FOV], 37 × 37 mm; matrix size, 256 × 256; repetition time, 25 ms; echotime, 5 ms;

acquisition time , 25.5 minutes; flip angle, 90°; 2 averages). A caudal presaturation of the neck arteries was applied. On MR-angiography source images (0.3-mm thickness) the confluence sinuum and the rostral end of the frontal cortex were identified. Sinus occlusion was given as percentage of slices without visible flow in the superior sagittalis sinus.

Middle cerebral artery occlusion in rats

Middle cerebral artery occlusion was induced in Wistar rats using the endovascular suture occlusion technique as described previously.[31,32] Male animals were randomized in 3 groups of 10 rats each, receiving prior to occlusion RNase (42 μg/kg), DNase (42 μg/kg), isotonic saline (control), or heparin (same dose as mentioned), respectively. Reperfusion was induced after 90 minutes by withdrawing the suture. MRI was performed after 24 hours using the 7-T unit described. High-resolution multislice proton- and T2-weighted double-contrast spin-echo imaging was used to map lesion and hemispheric volumes. A total of 8 coronal slices were acquired (thickness, 2 mm; FOV, 37 × 37 mm; matrix size, 512 × 256; TR, 3000 ms; TE1, 27 ms; TE2, 72 ms; TA, 25.5 minutes). Computer-aided planimetric assessment of the lesion and hemispheric volumes were performed, and lesion volumes were calculated as described previously.[32] To analyze absolute brain water content (percentage of H_2O), the convexities of the brains were separated and wet as well as dried weight of both hemispheres was measured. Calculation of percentage of H_2O is as follows: (wet weight − dry weight) ÷ wet weight × 100.[32] The increase of brain water content of the ischemic hemisphere was expressed as the difference in percentage of H_2O between both hemispheres. Since the ischemia-related increase in hemispheric water content is depending on infarct size, this value was divided by lesion volume (as determined on MRI) to calculate the edema-lesion ratio.

Measurement of the extravasation of Evans Blue dye was measured in 10 animals each from the control and RNase-treatment groups following the treatment protocol. Evans Blue dye (10%) was injected intravenously, and the animals were transcardially perfused 6 hours after middle cerebral artery occlusion to remove the intravascular dye. The brains were removed, sectioned coronally, and digitized. Evans Blue extravasation was quantified in regions of interest that were placed into the infarcted area and on corresponding positions on the contralateral hemisphere. Relative grayscale intensity was quantified using Image J software (National Institutes of Health, Bethesda, MD).

Immunolabeling and confocal microscopy

After middle cerebral artery occlusion and reperfusion, rat brains were retrogradely perfusued via the apex of the heart with 2% paraformaldehyde. After being exposed to increasing sucrose concentrations (10%, 20%, and 30% sucrose), the tissue samples were snap-frozen in liquid nitrogen and cryosections were prepared under the control of MRI data and based on the morphology of the infarcted areas. Immunolabeling and confocal microscopy were carried out as previously described.[33,34] In brief, following incubation with polyclonal antibodies against ZO-2 or claudin-5 and direct labeling with Cy3 monoclonal antibody against α-smooth muscle actin (Sigma), tissue sections were incubated with donkey anti-rabbit IgG directly coupled with Cy2 (Biotrend). Nuclei were stained with DAPI (Invitrogen).

A series of confocal optical sections were taken through the depth of the tissue sample at 0.5-μm intervals with the help of an SP2 confocal scanning laser microscope (Leica Microsystems, Bensheim, Germany). After signal-averaging of each image, an image restoration and 3D reconstruction using Imaris, the multichannel image processing software (Bitplane, Zürich, Switzerland), was carried out.[33,34] For quantitative analysis of ZO-2 labeling, 5 randomly selected fields, from either infarcted or undamaged cortexes, were scanned at 0.5-μm intervals, and from each field, 1 histogram of ZO-2 fluorescence intensity from 5 confocal sections was converted for calculation of ZO-2 signals.[35] The quantity of ZO-2 labeling was expressed as the percentage of surface area occupied by $ZO\text{-}2^+$ label per tissue area.

Statistical analysis

Results were expressed as the means (± SEM). The unpaired Student *t* test or analysis of variance (ANOVA) and subsequent multiple comparisons using the Dunn method were used for statistical analysis. Results were considered as statistically different at *P* values less than .05. For multiple comparisons between different groups of the in vivo models, we used ANOVA on ranks, followed by analysis with the Bonferroni *t* test. Differences between groups were considered significant at *P* values less than .05.

Results

Extracellular RNA mediates endothelial-cell hyperpermeability

Extracellular nucleic acids were tested for their influence on cellular permeability. Isolated RNA increased the flux of radiolabeled inulin across tight BMEC monolayers in a concentration-dependent manner with an onset at 25 μg/mL RNA. Artificial RNA such as poly-I:C or ssRNA significantly increased cellular permeability as well, reaching a maximal effect between 10 and 25 μg/mL, or at 0.25 μg/mL, respectively (Figure 1A). DNA at comparable concentrations did not increase cellular permeability significantly. After preincubation of RNA (3 hours) or poly-I:C with RNase (24 hours), permeability-inducing activities of both nucleic acids were abolished completely, whereas RNase itself did not influence cellular permeability (Figure 1B). The RNA equivalent quantity of nucleotide monophosphates did not influence the permeability of BMECs either. In the presence of an RNase inhibitor, which blocks RNaseA, RNaseB, and RNaseC, the flux across the BMEC monolayer was unchanged, and the permeability-inducing activity of RNA was even increased moderately (Figure 1C). Simultaneous addition of RNA and RNase to endothelial monolayers did not affect the permeability-inducing activity of the nucleic acid (Figure S1, available on the *Blood* website; see the Supplemental Materials link at the top of the online article). Moreover, electrical resistance across human umbilical vein endothelial-cell (HUVEC) monolayers was significantly decreased by RNA, particularly at concentrations higher than 50 μg/mL (Figure S2A). Due to the significantly higher quantities of endogenous RNase released by HUVECs compared with BMECs (Figure S2B), these differences in the effective dose of RNA may be explained.

Disintegration of intercellular tight junctions by RNA

Under quiescent conditions in cultured BMECs, the tight junction proteins ZO-1, ZO-2, occludin, claudin-5, and also VE-cadherin exhibited an intercellular continuous distribution by decorating intact cell-cell borders. RNA, poly-I:C, ssRNA, or heparin, but not DNA, provoked disintegration of junctional localization for the indicated proteins. Thus, staining for the indicated junctional proteins along the cell membranes became discontinuous or ruffled, and membranous invaginations projecting into the cytoplasma were formed (Figure 2). Western blot analysis of whole-cell lysate and the cytosolic and nucleic fractions demonstrated that the expression of all junctional proteins and of VE-cadherin was not changed in these fractions upon treatment with nucleic acids (Figure S3).

RNA- and heparin-induced cellular permeability is mediated by VEGF

Prior to permeability experiments, BMECs were preincubated 2 days with specific antisense oligonucleotides to VEGF-R2 or

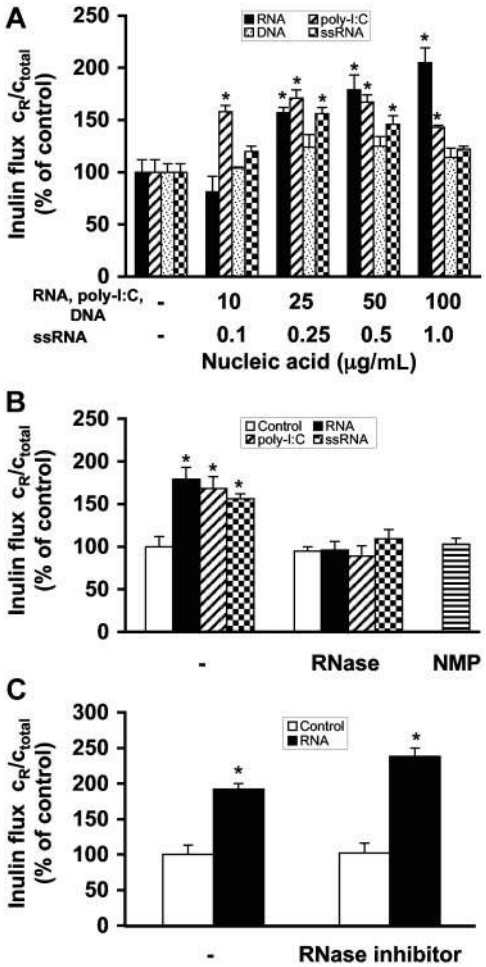

Figure 1. Induction of endothelial-cell permeability by extracellular nucleic acids. (A) Following addition of different concentrations of RNA, poly-I:C, DNA, or ssRNA to BMEC monolayers for 3 hours as indicated, permeability changes were quantitated by measuring the flux of [^{3}H]inulin.[29] (B) Permeability changes were analyzed in nontreated cells (control) or cells treated with RNA (50 μg/mL), poly-I:C (25 μg/mL), or ssRNA (0.25 μg/mL) as indicated in the absence (−) or presence of RNase or following addition of nucleotide monophosphates (NMPs; 50 μg/mL) instead of nucleic acids. (C) Permeability changes were measured after incubation of cells with RNA, as compared with control cultures (control) as indicated, in the absence ([minus) or presence of RNase inhibitor. Control flux determined after 3 hours was set to 100%, and values represent the mean (± SEM; n = 24) for each condition. *$P < .05$ compared with untreated cells.

VEGF-R1, respectively, which resulted in down-regulation of protein expression of the corresponding receptor as confirmed by Western blot analysis (Figure S4). RNA-induced permeability changes were blocked by the antisense oligonucleotide to VEGF-R2 or by a neutralizing antibody against VEGF, but not by the antisense oligonucleotide to VEGF-R1 (Figure 3A,B). Congruent results were obtained when poly-I:C, ssRNA or heparin were used as agonists. Moreover, scrambled (control) oligonucleotides against both VEGF-receptors were not effective (Figure 3A,B). As another control, the cellular permeability of epithelial CSG cells, which only express VEGF-R1,[36] was not influenced by RNA.

RNA-mediated release of VEGF is not induced at the transcriptional level

After treatment of BMECs for 24 hours with RNA, poly-I:C, ssRNA, or heparin (but not with DNA), an almost 2-fold increase of VEGF released into the culture medium was found (Figure S5A), whereas no increase of released VEGF over control was detectable after 3 hours (data not shown). In any case, no damage of cells by these agents occurred as demonstrated by a toxicity test (Table S1). Moreover, semiquantitative polymerase chain reaction (PCR) analysis indicated that after treating the cells with the mentioned agonists for 3 hours, the expression intensity of PCR products for VEGF isoforms remained unchanged (Figure S5B).

RNA-induced hyperpermeability does not involve activation of MAP kinases

Although Western blot analysis demonstrated that poly-I:C, but not RNA or ssRNA, induced the phosphorylation of the mitogen-activated protein (MAP) kinase p44/p42 and of the stress-activated protein kinase/Jun-terminal kinase (SAPK/JNK), but not of MAP kinase p38 (Figure S6A), inhibition of these MAP kinases by PD98959, SP600125, and SB203580, did not change RNA-, poly-I:C–, or ssRNA-induced permeability changes (Figure S6B). Furthermore, inhibition of phosphatidylinositol 3-kinase and of double-stranded RNA (dsRNA)–dependent protein kinase by wortmannin or aminopurine-2, respectively, did not inhibit RNA-mediated hyperpermeability. Only inhibition of the nitric-oxide synthase by NMMA abolished RNA-, poly-I:C-, or ssRNA-mediated permeability changes (Figure S6C). A toxicity test confirmed that the used inhibitors were not toxic to BMECs (Table S2).

RNA binding to VEGF

Binding of biotinylated RNA to $VEGF_{165}$ revealed a concentration-dependent and saturable kinetic, whereas binding to $VEGF_{121}$ (lacking the primary heparin-binding site) was hardly discernable. Maximal binding of $VEGF_{165}$ was reached at a concentration of 12.5 μg/mL biotinylated RNA (Figure 4A). Accordingly, other growth factors containing a heparin-binding domain like platelet derived growth factor or basic fibroblast growth factor exhibited similar binding characteristics, whereas placental growth factor-1, lacking a heparin-binding site, did not bind RNA. The binding of biotinylated RNA to $VEGF_{165}$ was competed by high concentrations of unlabeled RNA or heparin (Figure 4B).

Influence of RNase on sinus sagittalis superior thrombosis and focal cerebral ischemia

An in vivo model of $FeCl_3$-induced sinus sagittalis superior wall necrosis with concomitant thrombus and edema formation was applied to analyze the contribution of endogenous extracellular RNA in this cell-destructive situation and to assess the influence of RNase administration. In the saline (control) pretreatment group (absence of any additives), an average vessel occlusion rate of 95.7% (± 8%) was seen, with a decrease of this occlusion to 62% (± 26%) at postoperative day 1 and to 49% (± 26%) after 7 days (Figure 5A). Pretreatment with exogenous RNase, but not DNase, already decreased the extent of vessel occlusion significantly to 72% of control at day 0. On postoperative day 7, only 13.6% (± 6.2%) of the sinus sagittalis superior remained occluded in the RNase treatment group, reaching almost the same recanalization (< 10% occlusion) as observed in the heparin treatment group (Figure 5A). Mean arterial blood pressure and physiologic variables were within normal ranges in animals with sinus occlusion in all groups. RNase and heparin, but not DNase, increased the bleeding time 30 minutes after application as compared with vehicle, but reached initial values after 24 hours (Figure 5B).

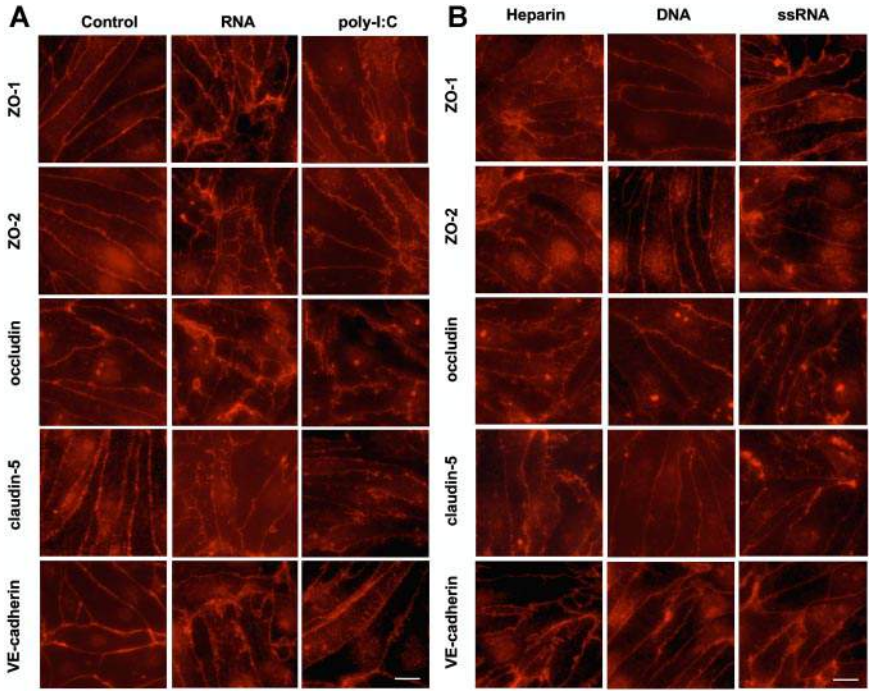

Figure 2. Disintegration of endothelial monolayers mediated by extracellular nucleic acids. Confluent BMECs, cultured on rat tail collagen I–coated coverslips, were incubated for 3 hours in the absence (control) or presence of RNA (50 μg/mL), poly-I:C (25 μg/mL), heparin (10 μg/mL), DNA (25 μg/mL), or ssRNA (0.25 μg/mL), fixed, and stained with the corresponding antibodies against the indicated junctional proteins. Note the disintegration of intercellular junctions and the changed cellular distribution of ZO-1, ZO-2, occludin, claudin-5, and VE-cadherin following treatment of cells with RNA, poly-I:C, heparin, and ssRNA, but not DNA. Scale bar equals 10 μm, magnification was 63×/1.32-0.6 (oil objective). Images were taken using a Wisitron Systems GmbH (Puchheim, Germany) and analysed by image-acquisition software MetaMorph, version 7 (Molecular Devices, Berkshire, United Kingdom).

Hematoxylin-eosin staining of paraffin-embedded brain sections prepared from saline-treated control rats demonstrated $FeCl_3$-induced thrombus formation and edema formation around the sinus sagittalis. RNase, but not heparin, prevented edema formation as demonstrated by the absence of fluid-filled area around vessels (Figure 5C), while thrombus formation was decreased in rats of both treatment groups. Interestingly, the extent of vessel occlusion as well as edema formation was also reduced by using an anti-VEGF antibody (78% ± 9%, 51% ± 13%, and 31% ± 18% after 1 hour, 24 hours, or 7 days, respectively) and reached nearly the same values as compared with the RNase treatment group. Hematoxylin-eosin staining of paraffin-embedded brain sections in which no perivascular edema formation was discernable confirmed these results (Figure S7). Moreover, pretreatment of animals with a low-molecular-weight factor XIIa inhibitor did not significantly alter the extent of vessel occlusion and edema formation compared with the control group (98% ± 3%, 74% ± 12%, or 38% ± 18% after 1 hour, 24 hours, or 7 days).

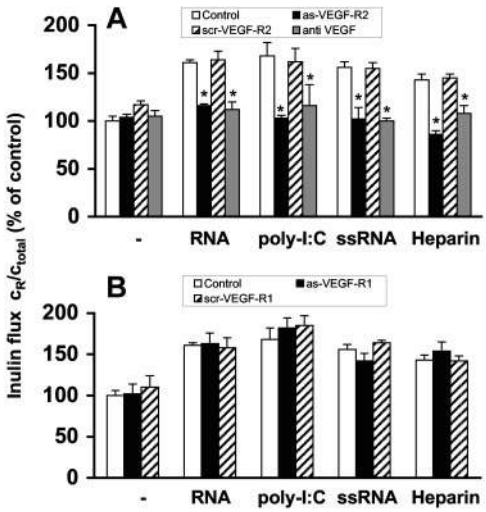

Figure 3. Induction of endothelial-cell permeability by RNA is mediated via VEGF. Confluent BMEC cultures were preincubated for 2 days with (A) antisense oligonucleotide to VEGF-R2 (as-VEGF-R2; 2 μM) or the scrambled nonsense oligonucleotide (scr-VEGF-R2; 2 μM). Permeability changes were analyzed in the absence of additives (−) or following treatment with RNA (50 μg/mL), poly-I:C (25 μg/mL), ssRNA (0.25 μg/mL), or heparin (10 μg/mL), and additionally in the presence of anti-VEGF antibody (10 μg/mL). Values represent the mean (± SEM; n = 24). *$P < .05$ compared with the corresponding control. (B) Alternatively, BMEC cultures were preincubated for 2 days with the antisense oligonucleotide to VEGF-R1 (as-VEGF-R1; 2 μM) or the scrambled nonsense oligonucleotide (scr-VEGF-R2; 2 μM) and treated as before. Flux determined after 3 hours in the absence of any added compound was set to 100%, and values represent the mean (± SEM; n = 9) for each condition. *$P < .05$ compared with the corresponding control value.

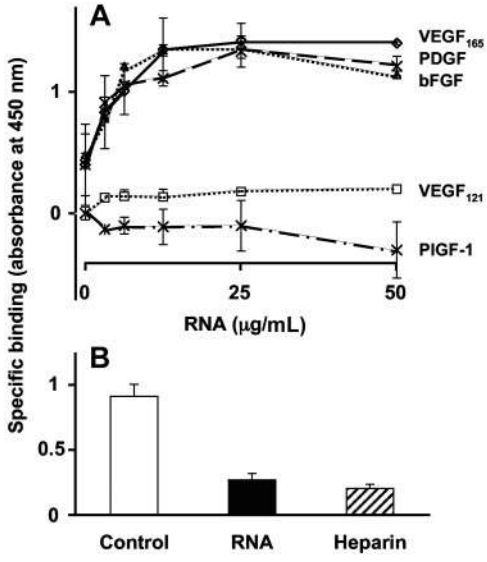

Figure 4. Direct binding of RNA to VEGF. (A) Binding of biotinylated RNA to immobilized $VEGF_{165}$, $VEGF_{121}$, platelet-derived growth factor (PDGF), basic fibroblast growth factor (bFGF), or placenta-derived growth factor (PlGF-1) was performed in a solid binding assay, and data are corrected for unspecific binding to BSA. (B) Binding of biotinylated RNA (6.25 μg/mL) to $VEGF_{165}$ was performed in the absence (control) or presence of 40-times molar excess of unlabeled RNA or heparin. Data represent the mean (± SEM; n = 4) of a typical experiment.

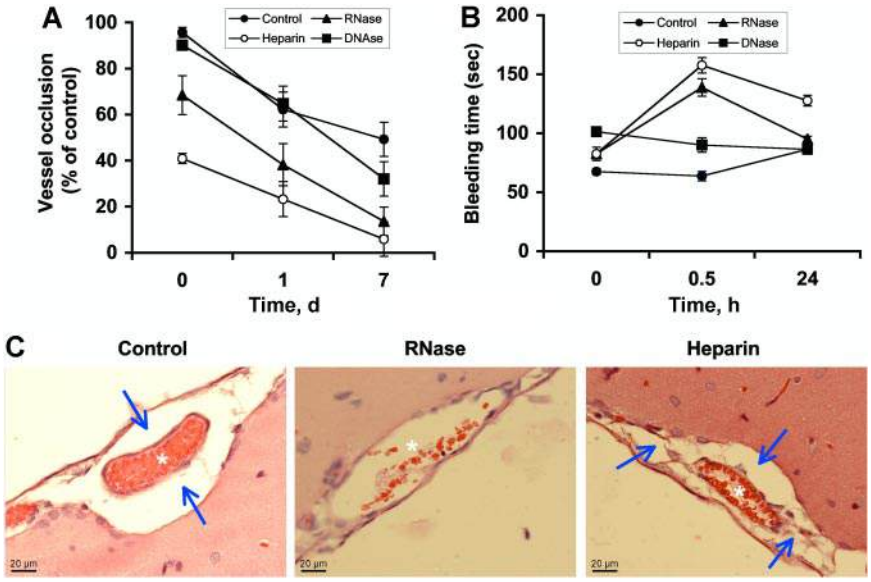

Figure 5. Influence of RNase pretreatment on venous thrombosis in rats. Vessel occlusion was induced by $FeCl_3$ exposure to the superior sagittalis sinus. At 30 minutes prior to the start of the experiment, animals were pretreated with either saline (Control), RNase, DNase, or heparin, respectively. At different time points after induction of thrombosis, (A) vessel occlusion rate and (B) bleeding times were determined. Values are expressed as the mean (± SEM; n = 12 for each animal group). (C) Hematoxylin-eosin staining of paraffin-embedded brain sections prepared from saline-treated (control), RNase-treated, or heparin-treated rats, respectively, was performed. Note the occluded vessel (∗) and massive perivascular edema formation (→) in the control, whereas in the RNase treatment group, greatly reduced vessel occlusion (∗) and hardly any edema were seen. In the heparin treatment group, no vessel occlusion (∗) is seen, whereas edema formation (→) remained. Slides were inspected with a DMRB Leica microscope, magnification was 40×/1.00-0.5 NA objective. Images were taken using a digital camera DFC300FX and image-acquisition software IM500 form Leica.

The influence of RNase administration on vasogenic brain edema formation during transient focal cerebral ischemia was studied using an in vivo stroke model. Compared with vehicle-treated animals, pretreatment with RNase resulted in a statistically significant reduction of brain edema, whereas treatment with DNase had no effect on edema formation (Figure 6A). Furthermore, RNase treatment resulted in a neuroprotective effect as demonstrated by a significantly reduced ischemic lesion volume (Figure 6B). To further visualize increased leakiness of the BBB in the in vivo stroke model, the extravasation of Evans Blue dye into ischemic tissue was estimated following transient middle cerebral artery occlusion for 90 minutes. As shown in Figure 6C, RNase pretreatment of the animals significantly reduced the blue staining of infarcted areas.

Immunoconfocal analysis revealed that the tight junction–associated protein ZO-2 is confined to intact vessels and undamaged cortex, and the ZO-2 area occupies 6.02% ± 1.18% of the normal tissue (Figure 7A,F). In the infarcted brain, ZO-2 was found to be dramatically reduced and comprised only 0.55% ± 0.36% of the infarcted tissue area (Figure 7B,F). Pretreatment of rats with RNase, but not with DNase or heparin, significantly preserved the amount of ZO-2. Similar results were obtained using immunoconfocal microscopy for claudin-5 (Figure S8), indicating that exogenous RNase confers vessel-protective activity.

Discussion

This study demonstrates that extracellular RNA and artificial RNA such as poly-I:C or ssRNA (but not DNA) increased the permeability of different endothelial-cell monolayers in a concentration-dependent manner, very similar to the activity of heparin. As compared with RNA, maximal permeability-inducing activity of ssRNA was already reached at much lower concentrations, indicating that structural differences between nucleic acids are important for their functional effects on BMECs. RNase-treated ribonucleic acids or nucleotide monophosphates had no influence on endothelial permeability, indicative for the requirement of polymeric nature of RNA species. Both micro- and macrovascular endothelial cells responded to RNA, whereas higher concentrations of RNA were required to increase cellular permeability across HUVECs. This was likely due to the fact that HUVECs produce and release appreciable quantities of RNase compared with BMECs. Simultaneous addition of RNase together with RNA did not, however, affect the activity of the nucleic acid, supporting the conclusion that extracellular RNA would be protected against degradation by binding to extracellular sites.

Increased paracellular permeability is known to correlate with disruption of tight junctions[37-39]: here, the permeability changes induced by RNA, poly-I:C, ssRNA, or heparin provoked disintegration of the tight junction proteins occludin or claudin-5, and of

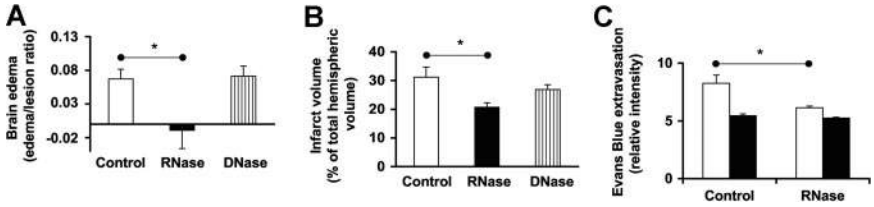

Figure 6. Influence of RNase on brain edema in a stroke model in rats. Middle cerebral artery occlusion was induced in rats using the endovascular suture occlusion technique. Prior to occlusion, animals were pretreated with either saline (control), RNAse, or DNase, respectively. (A) Hemispheric brain water content was measured using a wet-dry method, and the increase of brain water content of the ischemic hemisphere in relation to lesion volume was calculated (edema-lesion ratio); values represent the mean (± SEM; n = 10 in each animal group). (B) Ischemic lesion/infarct volume was determined by MRI (expressed as percentage of the volume of the hemisphere); values represent the mean (± SEM; n = 10 in each animal group). (C) To follow vascular leakage, Evans Blue extravasation following transient middle cerebral artery occlusion for 90 minutes was analyzed in the infarcted area (□) and in the corresponding contralateral hemisphere (■). Values represent the mean (± SEM; n = 5) in each panel. *$P < .05$.

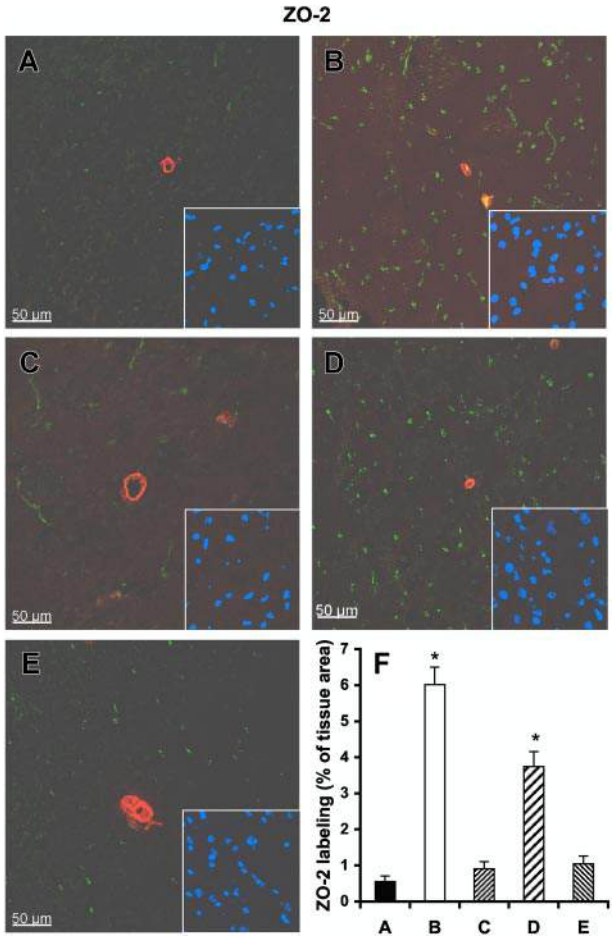

Figure 7. Influence of RNase on vessel integrity in infarcted brain tissue. Tissue cryosections of rat brains after middle cerebral artery occlusion were prepared from infarcted brain pretreated with either saline control (A), heparin (C), RNase (D), or DNase (E), or from noninfarcted brain areas (B). All sections were stained with a polyclonal antibody against ZO-2 (green fluorescence) and with a monoclonal antibody against α-smooth muscle actin (red fluorescence). Staining of the nuclei in the corresponding area is shown in the right corner of each panel. (F) Quantitative analysis of ZO-2 demonstrates that ZO-2 staining is dramatically reduced in infarcted brain areas (A), which is significantly restored after RNase pretreatment (D). Values represent the mean (± SEM; n = 6; *$P < .001$ versus group A = control), magnification was 40×/1.00-0.5 NA objective (Leica).

cytoskeleton-associated proteins ZO-1 and ZO-2.[40] Moreover, RNA treatment dislodged VE-cadherin from its association with tight junction proteins.[37] Extracellular RNA thereby induced restructuring of tight junctions that correlated with increased paracellular permeability, but without affecting protein expression. It is known that phosphorylation of junctional proteins leading to intracellular signaling might contribute to increased permeability.[41,42] The examination of the phosphorylation status of these proteins during RNA treatment will clarify whether this cellular mechanism is involved in BBB permeability changes.

Since RNA- (and heparin-) induced hyperpermeability was prevented by specific antisense oligonucleotides against VEGF-R2 or by antibodies to VEGF, the observed permeability changes are likely provoked by an indirect effect of RNA or heparin via VEGF itself. These results strongly indicate that the polyanionic character of natural and artificial RNA appears to be responsible for the mobilization and/or presentation of extracellularly bound VEGF, thereby enhancing its association with VEGF-R2. This contention was confirmed by direct binding of $VEGF_{165}$ to RNA. VEGF's heparin-binding domain is likely to be responsible for this medium-affinity interaction because other related growth factors presented a similar RNA-binding behavior, dependent on their heparin-binding domain. Although RNA had no effect on VEGF mRNA expression, after 24 hours of RNA treatment, appreciable amounts of VEGF were mobilized, indicative of the fact that extracellular RNA, like heparan sulfate or heparin, can promote VEGF binding to VEGF-R2. Whether extracellular RNA is thereby available to induce VEGF-dependent mitogenic signaling, tube formation, or VEGF-R2 phosphorylation[43-45] remains to be established.

Poly-I:C is known to activate Toll-like receptors, leading to the activation of dsRNA-dependent protein kinase, nuclear factor-κB, and several MAP kinases.[46-48] Although brain endothelial cells express Toll-like receptor-3, and poly-I:C (but not RNA) induced the phosphorylation of MAP kinases, activation of these pathways appears not to be involved in poly-I:C–induced permeability changes. Since inhibitors of the nitric oxide synthase prevented hyperpermeability, ribonucleic acids seem to mediate permeability changes at least in part via this signaling pathway. Our results further suggest that, despite the activation of Toll-like receptors with subsequent induction of particular signaling pathways in endothelial cells, these events are not responsible for the RNA-induced permeability changes described here.

Support for our contention that extracellular RNA, available during acute phases of tissue or vessel damage, may induce increased vascular permeability and edema formation linked to VEGF-dependent receptor activation, came from results of 2 animal models associated with massive vasogenic edema formation.

First, highly reproducible venous occlusion that leads to brain swelling, followed by massive cerebral edema with the possibility of pharmacologic recanalization, was generated by $FeCl_3$ treatment of the sinus sagittal is superior.[30] Like heparin, administration of RNase (but not DNase) resulted in a significant reduction of the occlusive thrombus as well as in a much shorter recanalization time. However, RNase but not heparin was effective in substantially reducing edema formation due to the fact that RNase prevented mobilization of VEGF by extracellular RNA, whereas heparin (like RNA) is known to activate the VEGF-dependent cellular signaling system. Furthermore, an antibody against VEGF reduced vessel occlusion and edema formation to a comparable level, as that of RNase pretreatment, indicative of the fact that both treatments affect the same permeability-inducing pathway. Together with our in vitro data, these observations support the contention that vascular permeability to a large extent appears to be operative through an extracellular RNA-VEGF axis. Extracellular RNA has recently been demonstrated by our group to serve as endogenous activator/cofactor for arterial thrombus formation via the contact phase pathway (including factor XII activation) of blood coagulation.[49] However, in the present venous occlusion model, no significant inhibition of vessel occlusion by a factor XIIa inhibitor was seen. These data not only indicate that RNA-dependent mechanisms are operative in a different way in arteries versus veins (using the same induction of vessel occlusion), but that intrinsic blood coagulation does not appreciably contribute to venous edema formation. Thus, in severely damaged (vascular) cells, RNA seems to be the predominant procoagulant and permeability-increasing cofactor in vivo, due to its immediate exposure and availability from damaged tissue, compared with DNA, the latter likely being protected by histones and its intranuclear localization.

Moreover, under these injury-related, pathologic conditions, locally generated RNA concentrations may reach levels that were effective in the in vivo and in vitro experiments of this study.

Despite the fact that blood plasma contains appreciable concentrations of RNase,[50] RNA released during vessel injury may directly bind to extracellular matrix sites or cell surfaces (M. Wygrecka et al, unpublished observations, March 2006) being protected from degradation by RNase. This contention is also supported by our in vitro experiments in which the permeability-increasing activity of RNA was not affected by RNase when both substances were simultanously incubated on endothelial cells. Only preincubation of RNA with RNase prior to the cellular assay destroyed the permeability-increasing function of the nucleic acid.

Secondly, a stroke model for transient focal cerebral ischemia within the middle cerebral artery territory was used to establish the influence of exogenous RNase on edema formation. Since edema formation here is likely be provoked by VEGF,[51] also known to be induced via hypoxia-inducible factors HIF-1 and HIF-2,[52-54] RNA and heparin would promote mobilization and stabilization of the growth factor due to their common polyanionic character and their interaction with VEGF. Although heparin and RNase were both effective as anticoagulants, the edema-protective effect of RNase cannot be duplicated by heparin, since the latter is a permeability-increasing factor as mentioned before. Thus, increased leakiness of Evans blue in infarcted brain areas was prevented only in the RNase treatment group.

Until now, the role of tight junctions in the control of vascular permeability to plasma components and circulating cells was supported by only a few studies.[55,56] Results in vivo by Witt et al first demonstrated that acute hypoxemia with initial reoxygenation for 10 minutes produced an increase in BBB permeability associated with alterations in tight junction protein expression.[57] Accordingly, staining for ZO-2 or claudin-5 was significantly reduced in sections prepared from infarcted areas comparison with noninfarcted regions. The lack of recognition of junctional proteins may be due to the disassembly of tight junctions, modifications like phosphorylation, or endocytosis of junctional proteins. As these junctions are responsible for the paracellular permeability across the BBB, our results additionally confirmed that counteraction of extracellular RNA was efficient to prevent increased leakiness of the BBB in infarcted areas. Thus, RNase treatment would serve as a useful novel and combined approach for antithrombotic treatment and reduction of vascular permeability or edema formation that might also prove to be neuroprotective.

Acknowledgments

We thank Bärbel Fühler and Jacqueline Hellwig for skillful technical assistance, and all other members of our laboratory for helpful discussions.

This work was supported by grants SFB-547, KFO-118 from the Deutsche Forschungsgemeinschaft (Bonn, Germany) to K.T.P., and from the Willy and Monika Pitzer Foundation (Bad Nauheim, Germany) to S.K.

Authorship

Contribution: S.F. planned and performed the majority of in vitro experiments and wrote the paper; T.G., M.W., and E.S. designed and performed the in vivo experiments regarding the stroke model and analyzed the respective data; C.W. and K.Z. designed and performed the in vivo experiments regarding the sinus thrombosis model and analyzed the respective data; S.K. performed the immunolabeling and confocal microscopy of brain sections; A.H. and S.H. did the resistance measurements of HUVECs; and K.T.P. designed and supervised the research and wrote the paper. S.F. and T.G. are equal first authors.

Conflict-of-interest disclosure: The authors declare no competing financial interests.

Correspondence: Klaus T. Preissner, Department of Biochemistry, Medical School, Justus-Liebig-Universität, Friedrichstrasse 24, D-35392 Giessen, Germany; e-mail: klaus.t.preissner@biochemie.med.uni-giessen.de.

References

1. Brightman MW, Reese TS. Junctions between intimately apposed cell membranes in the vertebrate brain. J Cell Biol. 1969;40:648-677.
2. Abbott NJ, Revest PA. Control of brain endothelial permeability. Cerebrovasc Brain Metab Rev. 1991;3:39-72.
3. Crone C, Olesen SP. Electrical resistance of brain microvascular endothelium. Brain Res. 1982;241:49-55.
4. Betz AL, Coester HC. Effect of steroids on edema and sodium uptake of the brain during focal ischemia in rats. Stroke. 1990;21:1199-1204.
5. Sampaola S, Nakagawa Y, Iannotti F, Cervos-Navarro J, Bonavita V. Blood-brain barrier permeability to micromolecules and edema formation in the early phase of incomplete continuous ischemia. Acta Neuropathologica. 1991;82:107-111.
6. Dvorak HF, Brown LF, Detmar M, Dvorak AM. Vascular permeability factor/vascular endothelial growth factor, microvascular hyperpermeability, and angiogenesis. Am J Pathol. 1995;146:1029-1039.
7. Baethmann A. Pathophysiological and pathochemical aspects of cerebral edema. Neurosurg Rev. 1978;1:85-100.
8. Schoch HJ, Fischer S, Marti HH. Hypoxia-induced VEGF expression causes vascular leakage in the brain. Brain. 2002;125:2549-2557.
9. Goldman CK, Bharara S, Palmer CA, et al. Brain edema in meningiomas is associated with increased vascular endothelial growth-factor expression. Neurosurg. 1997;40:1269-1277.
10. Senger DR, Ledbetter SR, Claffey KP, Papadopoulos-Sergiou A, Perruzzi CA, Detmar M. Stimulation of endothelial cell migration by vascular permeability factor/vascular endothelial growth factor through cooperative mechanisms involving αvβ3 integrin, osteopontin, and thrombin. Am J Pathol. 1996;149:293-305.
11. Ferrara N, Henzel WJ. Pituitary follicular cells secrete a novel Heparin-binding growth factor specific for vascular endothelial cells. Biochem Biophys Res Commun. 1989;161:851-858.
12. Connolly DT, Heuvelman DM, Nelson R, et al. Tumor vascular permeability factor stimulates endothelial cell growth and angiogenesis. J Clin Invest. 1989;84:1470-1478.
13. Senger DR, Dvorak AM, Peruzzi CA, Harvey VS, Dvorak HF. Tumor cells secrete a vascular permeability factor that promotes accumulation of ascites fluid. Science. 1983;219:983-985.
14. Mcdonald NQ, Hendrickson WA. A structural superfamily of growth factors containing a cystine knot motif. Cell. 1993;73:421-424.
15. Cross MJ, Dixelius J, Matsmoto T, Claesson-Welsh L. VEGF-receptor signal transduction. Trends Biochem Sci. 2003;28:488-494.
16. Robinson CJ, Stringer SE. The splice variants of vascular endothelial growth factor (VEGF) and their receptors. J Cell Sci. 2001;114:853-865.
17. Houck KA, Leung DW, Rowland AM, Winer J, Ferrara N. Dual regulation of vascular endothelial growth factor bioavailability by genetic and proteolytic mechanisms. J Biol Chem. 1992;267:26031-26037.
18. De Vries C, Escobedo JA, Ueno H, Houck K, Ferrara N, Williams LT. The fms-like tyrosine kinase, a receptor for vascular endothelial growth factor. Science. 1992;255:989-991.
19. Shibuya M. Structure and function of VEGF/VEGF-receptor system involved in angiogenesis. Cell Struct Funct. 2001;26:25-35.
20. Quinn TP, Peters KG, De Vries C, Ferrara N, Williams LT. Fetal liver kinase 1 is a receptor for vascular endothelial growth factor and is selectively expressed in vascular endothelium. Proc Natl Acad Sci U S A. 1993;90:7533-7537.
21. Veikkola T, Karkkainen M, Makinen T, Claesson-Welsh L, Alitalo K. Regulation of angiogenesis via vascular endothelial growth factor receptors. Cancer Res. 2000;60:203-212.
22. Wieczorek AJ, Rhyner C, Block LH. Isolation and characterization of an RNA-proteolipid complex assiciated with the malignant state in humans. Proc Natl Acad Sci U S A. 1985;82:3455-3459.
23. Kamm RC, Smith AG. Nucleic acid concentrations in normal human plasma. Clin Chem. 1972;18:519-522.
24. Kopreski MS, Benko FA, Kwak LW, Gocke CD. Detection of tumor messenger RNA in the serum of patients with malignant melanoma. Clin Cancer Res. 1999;5:1961-1965.

25. Chen X, Bnnefoi H, Pelte M-F, et al. Telomerase RNA as a detection marker in the serum of breast cancer patients. Clin Cancer Res. 2000;6:3823-3826.
26. Garcia-Olmo DC, Ruiz-Piqueras R, Garcia-Olmo D. Circulating nucleic acids in plasma and serum (CNAPS) and its relation to stem cells and cancer metastasis: state of the issue. Histol Histopathol. 2004;19:575-583.
27. Nakazawa F, Kannemeier C, Shibamiya A, et al. Extracellular RNA is a natural cofacozr for the (auto-)activation of Factor VII-activating protease (FSAP). Biochem J. 2005;385:831-838.
28. Reddi KK, Holland JF. Elevated serum ribonuclease in patients with pancreatic cancer. Proc Natl Acad Sci U S A. 1976;73:2308-2310.
29. Fischer S, Wiesnet M, Renz D, Schaper W. H_2O_2 induces paracellular permeability of porcine brain-drived microvascular endothelial cells by activation of the p44/42 MAP kinase pathway. Eur J Cell Biol. 2005;84:687-697.
30. Röttger C, Bachmann G, Gerriets T, et al. A new model of reversible sinus sagittalis superior thrombosis in the rat: magnetic resonance imaging changes. Neurosurg. 2005;57:773-579.
31. Gerriets T, Stolz E, Walberer M, et al. Noninvasive quantification of brain edema and the space-occupying effect in rat stroke models using magnetic resonance imaging. Stroke. 2004;35:566-571.
32. Gerriets T, Stolz E, Walberer M, et al. Complications and pitfalls in stroke models for middle cerebral artery occlusion: a comparison between the suture and the macrosphere model using magnetic resonance angiography. Stroke. 2004;35: 2372-2377.
33. Kostin S, Hein S, Bauer EP, Schaper J. Spatiotemporal development and distriution of the intercellular junctions in adult rat cardiomyocytes in culture. Circ Res. 1999;85:154-167.
34. Kostin S, Schaper J. Tissue-specific patterns of gap junctions in adult rat atrial and ventricular cardiomyocytes in vivo and in vitro. Circ Res. 2001;88:933-939.
35. Kostin S, Rieger M, Dammer S, et al. Gap junction remodeling and altered connexin43 expression in the failing human heart. Mol Cell Biochem. 2003;242:135-144.
36. Vogel C, Bauer A, Wiesnet M, et al. Flt-1, but not Flk-1 mediates hyperpermeability through activation of the PI3-K/Akt pathway. J Cell Physiol. 2007;212:236-243.
37. Kevil CG, Oshima T, Alexander B, Coe LL, Alexander JS. H2O2-mediated permeability: role of MAPK and occludin. Am J Physiol Cell Physiol. 2000;279:C21-C30.
38. Mark KS, Davis TP. Cerebral microvascular changes in permeability and tight junctions induced by hypoxia-reoxygenation. Am J Physiol Heart Circ Physiol. 2002;282:H1485-H1494.
39. Lee HS, Namkoong K, Kim D-H, et al. Hydrogen-peroxide-induced alterations of tight junction proteins in bovine brain microvascular endothelial cells. Microvasc Res. 2004;68:231-238.
40. Furuse M, Itoh M, Hirase T, et al. Direct association of occludin with ZO-1 and its possible involvement in the localization of occludin at tight junctions. J Cell Biol. 1994;127:1617-1626.
41. Staddon JM, Herrenknecht K, Smales C, Rubin LL. Evidence that tyrosine phosphorylation may increase tight junction permeability. J Cell Sci. 1995;108:609-619.
42. Tsukamoto R, Nigam SK. Role of tyrosine phosphorylation in the reassembly of occludin and other tight junction proteins. Am J Physiol. 1999; 276:F737-F750.
43. Ashikari-Hada S, Habuchi H, Kariya Y, Kimata K. Heparin regulates vascular endothelial growth factor165-dependent mitogenic activity, tube formation, and its receptor phophorylation of human endothelial cells: comparison of the effects of heparin and heparin odified heparins. J Biol Chem. 2005;280:31508-31515.
44. Gitay-Goren H, Soker S, Vlodavsky I, Neufeld G. The binding of vascular endothelial growth factor to its receptor is dependent on cell surface-associated heparin-like molecules. J Biol Chem. 1992; 267:6093-6098.
45. Ono K, Hattori H, Takeshita S, Kurita A, Ishihara M. Structural features in heparin that interact with VEGF(165) and modulate its biological activity. Glycobiology. 1999;9:705-711.
46. Doukas J, Cutler AH, Mordes JP. Polyinosinic: polycytidylic acid is a potent activator of endothelial cells. Am J Pathol. 1994;145:137-147.
47. Marui N, Offerman MK, Swerlick R, et al. Vascular cell adhesion molecule-1 (VCAM-1) gene transcription and expression are regulated through an antioxidant-sensitive mechanism in human vascular endothelial cells. J Clin Invest. 1994;92: 1866-1874.
48. Yang J, Xu Y, Zhu C, Hagan MK, Lawley T, Offerman MK. Regulation of adhesion molecule expression in Kaposi's sarcoma cells. J Immunol. 1994;152:361-373.
49. Kannemeier C, Shibamiya A, Nakzawa F, et al. Extracellular RNA constitutes a natural procoagulant cofactor in blood coagulation. Proc Natl Acad Sci U S A. 2007;104:6388-6393.
50. Landré JBP, Hewett PW, Olivot J-M, et al. Human endothelial cells selectively express large amounts of pancreatic-type ribonuclease (RNase 1). J Cell Biochem. 2002;86:540-552.
51. Kimura K, Nakase H, Tamaki R, Sakaki T. Vascular endothelial growth factor antagonist reduces brain edema formation and venous infarction. Stroke. 2005;36:1259-1263.
52. Folkman J. Therapeutic angiogenesis in ischemic limbs. Circulation. 1998;97:1108-1110.
53. Marti HH, Risau W. Systemic hypoxia changes the organ-specific distribution of vascular endothelial growth factor and its receptors. Proc Nat Acad Sci U S A. 1998;95:15809-15814.
54. Marti HH, Risau W. Angiogenesis in ischemic disease. Thromb Haemost. 1999;82:44-52.
55. Martin-Padura I, Lostaglio S, Schneemann M, et al. Junctional adhesion molecule, a novel member of the immunoglobulin superfamily that distributes at intercellular junctions and modulates monocyte transmigration. J Cell Biol. 1998;142: 117-127.
56. Pedram A, Razandi M, Levin ER. Deciphering vascular endothelial cell growth factor/vascular permeability factor signaling to vascular permeability. J Biol Chem. 2002;277:44385-44398.
57. Witt KA, Mark KS, Hom S, Davis TP. Effects of hypoxia-reoxygenation on rat blood-brain barrier permeability and tight junctional protein expression. Am J Physiol Heart Circ Physiol. 2003;285: H2820-H2831.